Liquid Crystals
Publication details, including instructions for authors and subscription information:
http://www.informaworld.com/smpp/title~content=t713926090

Induction of smectic layering in nematic liquid crystals using immiscible components III. The effect of lateral n-alkanoyl substituents on the thermotropic behaviour of 2,5-bis[4-(n-perfluoroheptyloctyloxy)benzoyloxy] toluene

Aaron C. Small; Diana K. Hunt; Coleen Pugh

To cite this Article Small, Aaron C. , Hunt, Diana K. and Pugh, Coleen(1999) 'Induction of smectic layering in nematic liquid crystals using immiscible components III. The effect of lateral n-alkanoyl substituents on the thermotropic behaviour of 2,5-bis[4-(n-perfluoroheptyloctyloxy)benzoyloxy] toluene', Liquid Crystals, 26: 6, 849 — 857

To link to this Article: DOI: 10.1080/026782999204534

URL: http://dx.doi.org/10.1080/026782999204534

Liquid Crystals, 1999, Vol. 26, No. 6, 849–857

Induction of smectic layering in nematic liquid crystals using immiscible components†
III. The effect of lateral *n*-alkanoyl substituents on the thermotropic behaviour of 2,5-bis[4′-(*n*-perfluoroheptyloctyloxy)benzoyloxy] toluene

AARON C. SMALL‡, DIANA K. HUNT and COLEEN PUGH*
Department of Polymer Science, The University of Akron, Akron,
Ohio 44325-3909, USA

(*Received 2 November 1998; accepted 1 December 1998*)

Lateral *n*-alkanoyl substituents were introduced at the benzylic position of 2,5-bis-[4′-(*n*-perfluoroheptyloctyloxy)benzoyloxy] toluene by free radical bromination followed by esterification with the corresponding potassium *n*-alkanoates. All of the transition temperatures of the resulting 2,5-bis[4′-(*n*-perfluoroheptyloctyloxy)benzoyloxy] benzyl *n*-alkanoates decrease relative to those of 2,5-bis[4′-(*n*-perfluoroheptyloctyloxy)benzoyloxy] toluene and with increasing length of the *n*-alkanoyl substituent. The SmC–SmA transition decreases the most, thereby stabilizing the SmA mesophase and destabilizing the SmC mesophase. In contrast to the well established concept that lateral substituents disrupt smectic layering, none of the 2,5-bis[4′-(*n*-perfluoroheptyloctyloxy)benzoyloxy] benzyl *n*-alkanoates exhibit a nematic mesophase.

1. Introduction

Lateral substituents decrease the length-to-breadth ratio of calamitic mesogens. Therefore, lateral substitution of a short mesogen with a bulky group generally prevents it from forming a liquid crystalline phase [1]. However, more extended mesogens can better tolerate a decrease in the length-to-breadth ratio, even if substitution is at the centre of the mesogen. In this case, the substituent depresses both the isotropization and melting temperatures of nematic liquid crystals [2–6]. Both linear and branched alkyl substituents generally depress isotropization more than melting temperatures, thereby reducing the nematic temperature range [2–6]. For example, if the central aromatic ring of 1,4-bis(4′-*n*-octyloxybenzoyloxy)benzene [6] is laterally substituted with *n*-alkyl groups (figure 1), the temperatures of the crystalline melting and nematic–isotropic transitions decrease with increasing length of the lateral substituent, until they converge to almost constant values [2]. This indicates that the length-to-breadth ratio also converges, which is confirmed by the alignment of long *n*-alkyl and *n*-alkoxy lateral substituents parallel to the mesogen [7]. This parallel alignment enables the molecule to maintain a more rod-like shape and maximize packing.

Extended mesogens laterally substituted with aromatic groups may also exhibit nematic mesophases, especially

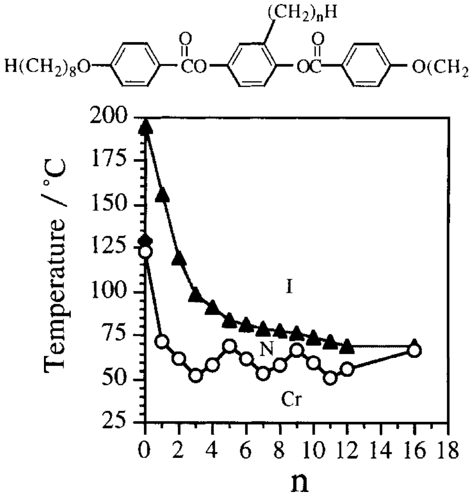

Figure 1. Dependence of the transition temperatures from the crystalline (○), smectic C (◆) and nematic (▲) phases of 2-*n*-alkyl-1,4-bis[4′-(*n*-octyloxy)benzoyloxy] benzenes as a function of the length of the *n*-alkyl lateral substituent [2, 6].

---

*Author for correspondence; e-mail: cpugh@polymer.uakron.edu.usa

†Part II see ref. [25]

‡Current address: University of Michigan, Department of Chemistry, Ann Arbor, Michigan 48109-1055, USA.

Journal of Liquid Crystals ISSN 0267-8292 print/ISSN 1366-5855 online ©1999 Taylor & Francis Ltd
http://www.tandf.co.uk/JNLS/lct.htm
http://www.taylorandfrancis.com/JNLS/lct.htm

if the aromatic substituent is connected through a spacer or flexible linkage [8, 9]. The aromatic substituents also depress isotropization more than melting, often to the extent that the nematic mesophase is monotropic [8]. Nevertheless, many of these compounds organize into smectic layers if the spacer is sufficiently flexible and/or the lateral aromatic group is further substituted with an *n*-alkyl or *n*-alkoxy group [9].

Since lateral substituents increase the molar volume and decrease the packing density of the mesogens [3], lateral substitution at the centre of the mesogen hinders the formation of smectic mesophases [1–6, 10]. For example, in contrast to unsubstituted 1,4-bis(4′-*n*-octyloxybenzoyloxy)benzene, none of the 2-*n*-alkyl-1,4-bis-(4′-*n*-octyloxybenzoyloxy)benzenes exhibit a smectic phase (figure 1) [2]. The introduction of lateral substituents into the mesogens of terminally attached side chain liquid crystalline polymers (SCLCPs) also depresses their transition temperatures and tends to suppress crystallization [11]. When the spacer is short, it tends to convert smectic mesophases into nematic mesophases or amorphous glasses [8]. In contrast to low molar mass liquid crystals (LMMLCs), small halide and methyl substituents [12], and flexible *n*-alkoxy [13] and *n*-alkanoyl [14] substituents generally depress melting more than isotropization of nematic main chain liquid crystalline polymers. This broadens the temperature range of the nematic mesophase or converts monotropic to enantiotropic mesophases. However, bulky substituents such as phenylsulphonyl [15], phenyleneimine [16] and chiral alkoxy [17] groups tend to depress isotropization more than melting, eliminate smectic mesophases, and convert enantiotropic nematic mesophases into monotropic phases.

In addition to using lateral substituents to convert smectic mesophases into nematic mesophases, few concepts have been developed for converting the type of mesophase(s) exhibited by liquid crystalline compounds, even though LMMLCs have been known since 1888 [18]. We are therefore establishing additional chemical tools for transforming the mesophases exhibited by both LMMLCs and SCLCPs. The most significant transformation is from nematic to smectic mesophases. We recently demonstrated that both nematic LMMLCs and polynorbornenes with laterally attached 1,4-bis-(4′-*n*-alkoxybenzoyloxy)benzene mesogens can be forced to order into smectic layers by terminating their *n*-alkoxy substituents with immiscible fluorocarbon segments (tables 1 and 2, respectively) [19, 20]. SCLCPs with laterally attached mesogens are the most challenging system possible for inducing smectic layering since lateral attachment of the mesogens to a polymer backbone had previously precluded smectic layering; both the molecular architecture [21] and the use of only a short spacer [22] disfavour smectic mesomorphism.

Table 1. Thermal transitions and thermodynamic parameters of 2,5-bis[4′-(*n*-perfluoroalkylalkoxy)benzoyloxy] toluenes [20]. Cr = crystalline, SmC = smectic C, SmA = smectic A, I = isotropic.

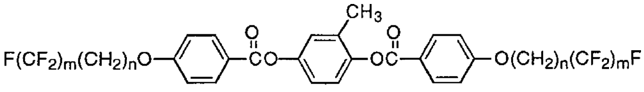

n	m	Phase transition temperature/°C (ΔH/kJ mol^{-1})[a]		
4	6	Cr 110 (44.1)	SmC 205 (0.46)	SmA 214 (8.76) I
5	6	Cr 101 (23.9)	SmC 197 (0.43)	SmA 208 (10.9) I
6	6	Cr 102 (48.9)	SmC 200 (0.46)	SmA 204 (10.4) I
8	6	Cr 104 (50.4)	SmC 190 (0.60)	SmA 193 (9.96) I
4	7	Cr 124 (45.1)	SmC 215 (0.69)	SmA 222 (6.67) I
5	7	Cr 119 (35.7)	SmC 208 (0.89)	SmA 216 (8.38) I
6	7	Cr 130 (45.5)	SmC 206 (0.63)	SmA 212 (6.78) I
8	7	Cr 120 (51.5)	SmC 199 (0.75)	SmA 200 (7.70) I
4	8	Cr 132 (46.8)	SmC 218 (1.10)	SmA 226 (8.66) I
5	8	Cr 122 (32.6)	SmC 214 (1.30)	SmA 221 (8.12) I
6	8	Cr 130 (58.5)	SmC 211 (1.45)	SmA 217 (8.88) I
8	8	Cr 124 (55.5)	SmC 201 (1.59)	SmA 205 (9.20) I

[a] Observed on heating.

Table 2. Thermal transitions and thermodynamic parameters of poly{5-[2′,5′-bis[4″-(*n*-perfluoroalkylalkoxy)benzoyloxy]-benzyloxycarbonyl] bicyclo[2.2.1] hept-2-ene}s [20]. g = glass, SmC = smectic C, SmA = smectic A, I = isotropic.

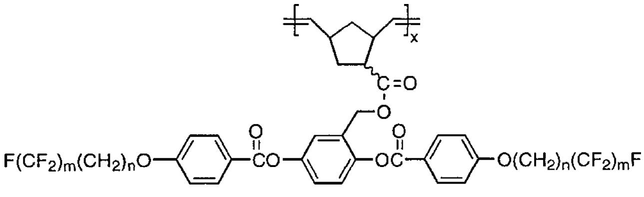

n	m	Phase transitions temperature/°C (ΔH/kJ mru^{-1})[a]		
4	6	g 106	SmC 227 (6.97)	SmA 234 (4.09) I
5	6	g 96	SmC 228[b]	SmA 231 (4.42) I
6	6	g 90	SmC 216[b]	SmA 223 (4.36) I
8	6	g 77	SmC 213[b]	SmA 216 (4.22) I
4	7	g 90	SmC 242 (3.21)	SmA 251 (0.52) I
5	7	g 96	SmC 239[b]	SmA 248 (4.35) I
6	7	g 93	SmC 230[b]	SmA 236 (3.56) I
8	7	g 97	SmC 228[b]	SmA 232 (3.45) I
4	8	g 93	SmC 251[b]	SmA 264 (3.87) I
5	8	g 93	SmC 258[b]	SmA 262 (3.81) I
6	8	g 98	SmC 250[b]	SmA 261 (3.78) I
8	8	g 98	SmC 231[b]	SmA 234 (0.69) I

[a] Observed on heating.

[b] Transition detected only by polarized optical microscopy.

Nevertheless, the hydrocarbon/fluorocarbon pair was the most promising combination we could choose to induce smectic layering. Aliphatic hydrocarbons and fluorocarbons are highly immiscible, with the largest known endothermic heats of mixing [23]. Microsegregation of the hydrocarbon and fluorocarbon is apparently so strong that the influence of the polymer backbone is minimal. That is, the polymers' transition temperatures (table 2) are similar to those of the low molar mass model compounds (table 1), with only the melting transition being replaced by a glass transition [20]. Consequently, these low molar mass model compounds, containing *n*-alkoxy substituents terminated with fluorocarbon segments, may be the most challenging system possible for disrupting smectic layering and converting smectic mesophases to a nematic mesophase. Therefore, we are testing the limits of the well-established concept that lateral substituents disrupt smectic layering, by determining if it is possible to convert the SmC and SmA mesophases of 2,5-bis[4′-(*n*-perfluoroheptyloctyloxy)benzoyloxy] toluene into a nematic mesophase, and if so, how bulky of a substituent is needed. This paper describes the synthesis and thermotropic behavior of 2,5-bis[4′-(*n*-perfluoroheptyloctyloxy)benzoyloxy] benzyl *n*-alkanoates, in which the central ring of 2,5-bis[4′-(*n*-perfluoroheptyloctyloxy)benzoyloxy] benzene is substituted with *n*-alkanoyl groups (see the scheme).

2. Results and discussion

As outlined in the scheme, the 2,5-bis[4′-(*n*-perfluoroheptyloctyloxy)benzoyloxy] benzyl *n*-alkanoates were synthesized from 2,5-bis[4′-(*n*-perfluoroheptyloctyloxy)benzoyloxy] toluene [20] by free radical bromination at the benzylic position using *N*-bromosuccinimide (NBS) in the presence of 2,2′-azobisisobutyronitrile (AIBN), followed by phase transfer catalyzed esterification with the corresponding potassium *n*-alkanoates. We started with 2,5-bis[4′-(*n*-perfluoroheptyloctyloxy)benzoyloxy]-toluene because it is one of the most soluble and least expensive compounds in table 1 to synthesize. The final yields were low due to difficulty in isolating the product from unreacted starting materials because of the similar solution and solid-state properties of the *n*-alkanoate products and components of the starting benzyl bromide mixture. Although we were able to isolate pure product by column chromatography using a gradient solvent system, much of the remaining product elutes with the benzyl bromide and 2,5-bis[4′-(*n*-perfluoroheptyloctyloxy)benzoyloxy] toluene due to their similar R_f values.

Figure 2 presents the differential scanning calorimetry (DSC) traces of the 2,5-bis[4′-(*n*-perfluoroheptyloctyloxy)benzoyloxy] benzyl *n*-alkanoates obtained on heating and on cooling at 10°C $\min^{-1}$; all of the DSC traces are normalized relative to each other. Table 3 summarizes their equilibrium thermotropic behavior. The data obtained on heating are from samples that are at thermodynamic equilibrium, and represent samples crystallized from solution and/or from the melt after annealing at room temperature. Since most of these compounds crystallize slower than the timescale of the DSC experiment, crystallization from the melt is incomplete during the cooling scan; only the *n*-hexanoate and *n*-octanoate derivatives have identical first and subsequent heating

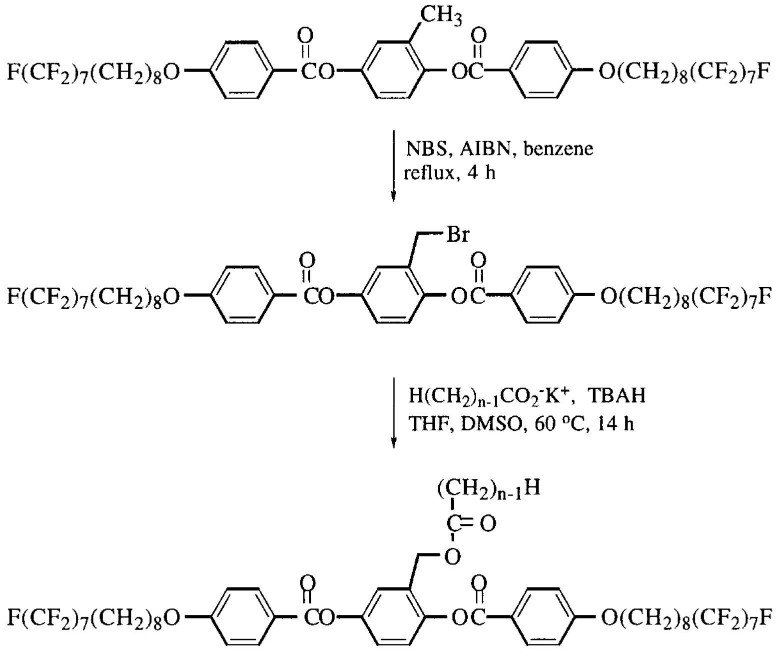

Scheme. Synthesis of 2,5-bis[4′-(*n*-perfluoroheptyloctyloxy)benzoyloxy] benzyl *n*-alkanoates (n = 2–13).

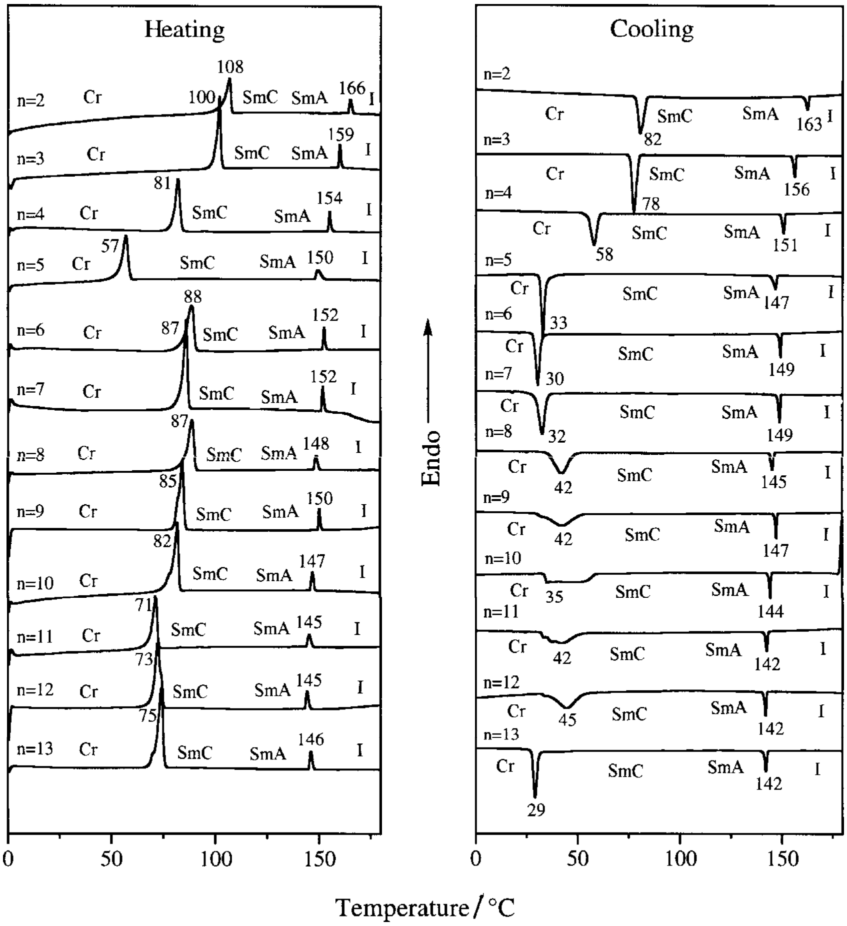

Figure 2. Normalized DSC traces of the 2,5-bis[4′-(*n*-perfluoroheptyloctyloxy)benzoyloxy] benzyl *n*-alkanoates (n = 2–13) observed on heating and on cooling at 10°C $\min^{-1}$.

scans. All other samples crystallize completely only after annealing at room temperature for several days. With the exception of the *n*-pentanoate, *n*-nonanoate and *n*-undecanoate derivatives, the annealed samples attain the same melting temperature and corresponding change in enthalpy as those compounds crystallized from solution.

The representative polarized optical micrographs presented in figure 3 confirm that all of the 2,5-bis[4′-(*n*-perfluoroheptyloctyloxy)benzoyloxy] benzyl *n*-alkanoates exhibit SmC and SmA mesophases. In contrast to the 2,5-bis[4′-(*n*-perfluoroalkylalkoxy)benzoyloxy] toluenes in table 1 [20], it is not necessary to pretreat the glass slides with a hydrocarbon film in order to prevent macroscopic homeotropic alignment and thereby observe the focal-conic fan texture of the SmA mesophase. This is consistent with the higher viscosity of laterally substituted liquid crystals compared with the corresponding unsubstituted compounds and those with smaller substituents [3]. The 2,5-bis[4′-(*n*-perfluoroheptyloctyloxy)benzoyloxy] benzyl *n*-alkanoates tend to exhibit both the homeotropic and focal-conic fan textures, which are the two natural textures of the SmA mesophase [24], in the same sample preparation, figure 3(*a*). When the samples are cooled into the SmC mesophase, figure 3(*b*), the homeotropic regions become schlieren, whereas the fans of the focal-conic fan regions become broken.

Comparison of tables 1 and 3 demonstrates that the introduction of a linear *n*-alkanoyl substituent at the benzylic position of 2,5-bis[4′-(*n*-perfluoroheptyloctyloxy)benzoyloxy] toluene does not convert the SmC and SmA mesophases into a nematic mesophase, even when the *n*-alkanoyl substituent is thirteen carbons long. None of the 2,5-bis[4′-(*n*-perfluoroheptyloctyloxy)benzoyloxy]-benzyl *n*-alkanoates exhibit a nematic mesophase; all twelve compounds exhibit a Cr–SmC–SmA–I phase sequence.

Tables 1 and 3 also list the enthalpy changes associated with the phase transitions of all the compounds. As discussed previously [20], the change in enthalpy of the various transitions of the 2,5-bis[4′-(*n*-perfluoroalkylalkoxy)benzoyloxy] toluenes (table 1) indicate that the aliphatic hydrocarbon segments disorder primarily at the melting transition, whereas the fluorocarbon segments

Table 3. Thermal transitions and thermodynamic parameters of 2,5-bis[4′-(*n*-perfluoroheptyloctyloxy)benzoyloxy] benzyl *n*-alkanoates (n = 2–13). Cr = crystalline, SmC = smectic C, SmA = smectic A, I = isotropic.

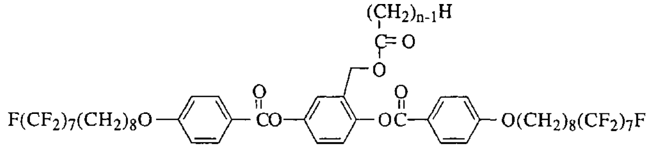

	Phase transition temperature/°C (ΔH/kJ mol^{-1})					
n	Heating			Cooling		
2	Cr 108 (33.4)	SmC 135[a]	SmA 166 (5.02) I	I 163 (5.19)	SmA 131[a]	SmC 82 (29.2) Cr
3	Cr 100 (41.7)	SmC 122[a]	SmA 159 (6.70) I	I 156 (6.77)	SmA 117[a]	SmC 78 (36.2) Cr
4	Cr 81 (39.9)	SmC 106[a]	SmA 154 (6.39) I	I 151 (6.68)	SmA 102[a]	SmC 58 (28.3) Cr
5	Cr 57 (46.5)	SmC 100[a]	SmA 150 (6.52) I	I 147 (6.55)	SmA 95[a]	SmC 33 (36.2) Cr
6	Cr 88 (57.5)	SmC 103[a]	SmA 152 (6.56) I	I 149 (6.73)	SmA 98[a]	SmC 30 (33.4) Cr
7	Cr 87 (65.4)	SmC 101[a]	SmA 152 (8.16) I	I 149 (8.52)	SmA 96 (0.487)	SmC 32 (42.0) Cr
8	Cr 87 (53.0)	SmC 98[a]	SmA 148 (5.76) I	I 145 (5.90)	SmA 92[a]	SmC 42 (40.8) Cr
9	Cr 85 (54.0)	SmC 101[a]	SmA 150 (6.23) I	I 147 (6.51)	SmA 95 (0.294)	SmC 42 (37.8) Cr
10	Cr 82 (62.1)	SmC 96[a]	SmA 147 (6.96) I	I 144 (7.25)	SmA 92[a]	SmC 35 (50.1) Cr
11	Cr 71 (46.0)	SmC 93 (0.127)	SmA 145 (6.46) I	I 142 (6.70)	SmA 90 (0.114)	SmC 42 (37.8) Cr
12	Cr 73 (64.2)	SmC 92 (0.187)	SmA 145 (7.40) I	I 142 (7.59)	SmA 90 (0.0335)	SmC 45 (42.0) Cr
13	Cr 75 (70.0)	SmC 94 (0.230)	SmA 146 (7.72) I	I 142 (7.87)	SmA 90 (0.421)	SmC 29 (37.2) Cr

[b] Transition detected only by polarized optical microscopy.

disorder primarily at the SmC–SmA transition. That is, the change in enthalpy of crystalline melting is essentially constant as a function of the fluorocarbon length for a given hydrocarbon, but appears to increase with an odd–even alternation as the hydrocarbon length increases. The change in enthalpy of the SmC–SmA transition is invariant to changes in the hydrocarbon length for a given fluorocarbon, but increases as the length of the fluorocarbon increases; the change in enthalpy of isotropization is independent of both hydrocarbon and fluorocarbon length.

The change in enthalpy of isotropization of the 2,5-bis[4′-(*n*-perfluoroheptyloctyloxy)benzoyloxy] benzyl *n*-alkanoates are similar to that of 2,5-bis[4′-(*n*-perfluoroheptyloctyloxy)benzoyloxy] toluene ($\Delta H_{\mathrm{i}} = 7.70\,\mathrm{kJ\,mol^{-1}}$), and are independent of the length of the *n*-alkanoyl substituent. In contrast, the change in enthalpy of the SmC–SmA transition is smaller than that for the parent compound, and the transition is therefore difficult to detect by DSC (figure 2). The change in enthalpy of crystalline melting of the laterally substituted derivatives generally increases as the length of the *n*-alkanoyl substituent increases. It is greater than that of 2,5-bis[4′-(*n*-perfluoroheptyloctyloxy)benzoyloxy] toluene ($\Delta H_{\mathrm{m}} = 51.5\,\mathrm{kJ\,mol^{-1}}$) when the *n*-alkanoyl substituent is at least six carbons long. This indicates that the lateral *n*-alkanoyl substituents also disorder at the melting transition, and that the lateral substituents may segregate and co-crystallize with the hydrocarbon portion of the *n*-alkoxy substituents when the lateral *n*-alkanoyl substituent contains at least five methylenic units.

Figure 4 plots the transition temperatures of the 2,5-bis[4′-(*n*-perfluoroheptyloctyloxy)benzoyloxy] benzyl *n*-alkanoates as a function of the number of carbons in the lateral *n*-alkanoyl substituent; the corresponding transitions of the unsubstituted 2,5-bis[4′-(*n*-perfluoroheptyloctyloxy)benzoyloxy] toluene are shown at n = 0 for comparison. Substitution of 2,5-bis[4′-(*n*-perfluoroheptyloctyloxy)benzoyloxy] toluene at the benzylic position with an acetate group depresses crystalline melting slightly and isotropization more so, but causes an especially large decrease of the SmC–SmA transition. This stabilizes the SmA mesophase significantly relative to the SmC mesophase by increasing the temperature range over which the SmA mesophase is observed, and decreasing the temperature range of the SmC mesophase. All of the transition temperatures continue to decrease as the length of the *n*-alkanoyl substituent increases, although the rate of decrease levels off when n ⩾ 6. The temperature windows of the SmC and SmA mesophases level off at 20 and 50°C, respectively, when n ⩾ 6.

3. Conclusions

Microsegregation of the hydrocarbon and fluorocarbon segments of 2,5-bis[4′-(*n*-perfluoroheptyloctyloxy)benzoyloxy] toluene is apparently so strong that a lateral *n*-alkanoyl substituent is not large enough to disrupt

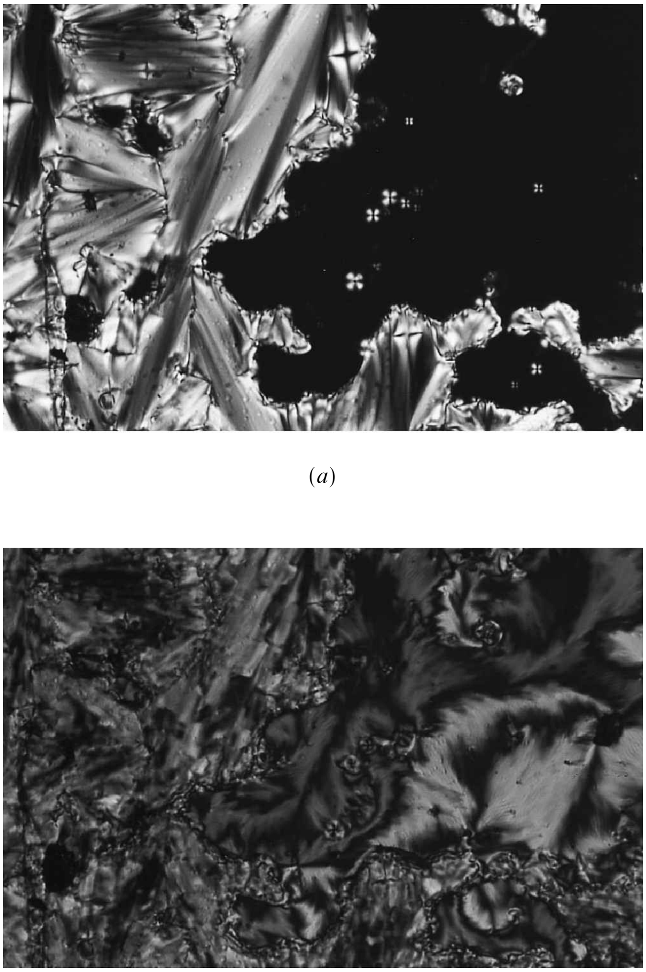

(*a*)

(*b*)

Figure 3. Polarized optical micrographs (200×) observed on cooling 2,5-bis[4′-(*n*-perfluoroheptyloctyloxy)benzoyloxy]-benzyl propionate from the isotropic melt: (*a*) 156°C, SmA focal-conic fan and homeotropic textures; (*b*) 112°C, SmC broken focal-conic fan and schlieren textures.

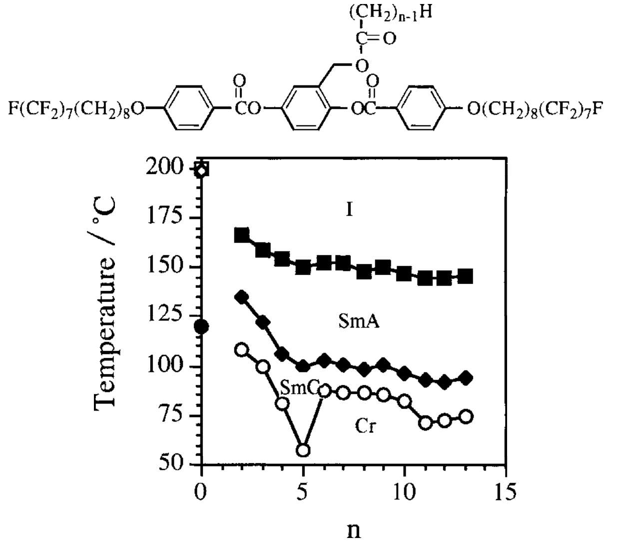

Figure 4. Dependence of the transition temperatures from the crystalline (○), smectic C (◆) and smectic A (■) phases of 2-*n*-alkyl-1,4-bis[4′-(*n*-octyloxy)benzoyloxy]-benzenes as a function of the number of carbons in the *n*-alkanoate lateral substitutent. The transitions from the crystalline (●), smectic C (◇) and smectic A (□) phases of the unsubstituted 2,5-bis[4′-(*n*-perfluoroheptyloctyloxy)-benzoyloxy] toluene are shown at n = 0 for comparison.

smectic layering and convert the SmC and SmA mesophases into a nematic mesophase. Instead, the lateral substituent stabilizes the SmA mesophase by depressing the SmC–SmA transition temperature more than that of melting and of isotropization. The transition temperatures level off when the *n*-alkanoyl substituent is at least six carbons long. This is consistent with other laterally substituted liquid crystals, in which the long *n*-alkyl and *n*-alkoxy lateral substituents align parallel to the mesogen [7]. The enthalpy of melting of the 2,5-bis[4′-(*n*-perfluoroheptyloctyloxy)benzoyloxy] benzyl *n*-alkanoates increases with increasing length of the substituent, even when it contains more than six carbons. This indicates that the lateral *n*-alkanoyl substituents reinforce microsegregation of the hydrocarbon and fluorocarbon portions of the molecule when $n \geq 6$, presumably by co-crystallization of the lateral *n*-alkanoyl substituent with the hydrocarbon segment of the terminal *n*-alkoxy substituent(s).

4. Experimental

4.1. *Materials*

Butyric acid (> 99%), decanoic acid (> 99%), heptanoic acid (99%), lauric acid (99.5%), octanoic acid (> 99.5%) and potassium acetate (> 99%) were used as received from Aldrich. Hexanoic acid (> 99%), pentanoic acid (99%) and tridecanoic acid (99%) were used as received from Sigma. Nonanoic acid (Alfa 98%), propionic acid (MCB, 99%), tetrabutylammonium hydrogen sulfate (TBAH, Acros, 98%) and undecanoic acid (Acros, 99%) were also used as received. 2,2′-Azobisisobutyronitrile (AIBN, Kodak, 99%) was recrystallized from methanol below 40°C. *N*-bromosuccinimide (NBS, Aldrich, 99%) was recrystallized from water. Dimethylsulfoxide (DMSO, Fisher) was distilled from CaH_2 under N_2. Reagent grade tetrahydrofuran (THF) was dried by distillation from purple sodium benzophenone ketyl under nitrogen. 2,5-Bis[4′-(*n*-perfluoroheptyloctyloxy)benzoyloxy] toluene was prepared as previously reported [20]. All other reagents and solvents were commercially available and used as received.

4.2. *Techniques*

Unless noted otherwise, all reactions were performed under a nitrogen atmosphere. ^{1}H NMR spectra (δ, ppm) were recorded on a Bruker AM-360 (360 MHz) spectrometer. All spectra were recorded in $CDCl_3$ with TMS as an internal standard. The thermotropic behaviour of all of the compounds was determined by a combination of DSC and polarized optical microscopy. A Perkin-Elmer DSC-7 instrument was used to determine the thermal transitions at 10°C min^{-1}. The endothermic and exothermic peaks were read at their maximum and minimum energies, respectively. Both enthalpy changes and transition temperatures were determined using indium as the calibration standard. All of the samples were initially heated three times and cooled twice; their equilibrium transition temperatures and enthalpies were subsequently determined through extensive annealing and quenching studies. A Leitz Laborlux 12 Pol S polarized optical microscope (magnification 200×) equipped with a Mettler FP82 hot stage and a Mettler FP90 central processor was used to observe the thermal transitions and to analyse the anisotropic textures [24]. Thin samples were prepared by melting a minimum amount of compound between a clean glass slide and a cover slip, and rubbing the cover slip with a spatula.

4.3. *Synthesis*

4.3.1. *2,5-Bis[4′-(n-perfluoroheptyloctyloxy)benzoyloxy]-benzyl bromide*

A solution of 2,5-bis[4′-(*n*-perfluoroheptyloctyloxy)-benzoyloxy] toluene (6.9 g, 5.2 mmol), AIBN (39 mg, 0.24 mmol) and NBS (1.7 g, 9.4 mmol) in benzene (21 ml) was heated under reflux for 4 h. The resulting orange mixture was then poured into 5% aq sodium bisulphite (50 ml), and extracted three times with CH_2Cl_2 (200 ml total). The organic layers were separated, and the solvent removed using a rotary evaporator. The slightly orange residue was recrystallized from a mixture of ethanol (100 ml) and toluene (36 ml) to yield 6.6 g (90%) of white solid containing 78% 2,5-bis[4′-(*n*-perfluoroheptyloctyloxy)benzoyloxy] benzyl bromide (71% overall yield), 13% 2,5-bis[4′-(*n*-perfluoroheptyloctyloxy)benzoyloxy]-toluene and 9% 2,5-bis[4′-(*n*-perfluoroheptyloctyloxy)-benzoyloxy] benzyl dibromide. This product mixture was used without further purification. ^1H NMR: 1.39 (m, $[C\mathit{H}_2]_3$, 12 H), 1.50 ($C\mathit{H}_2CH_2CH_2O$, 4 H), 1.61 (m, $C\mathit{H}_2CH_2CF_2$, 4 H), 1.83 (m, $C\mathit{H}_2CH_2O$, 4 H), 2.05 (m, $C\mathit{H}_2CF_2$, 4 H), 4.06 (m, $OC\mathit{H}_2$, 4 H), 4.45 (s, $C\mathit{H}_2Br$), 6.99 (dd, 4 aromatic H *ortho* to OCH_2), 7.33 (m, 3 aromatic H of central ring), 8.17 (dd, 4 aromatic H *ortho* to CO_2Ar). In addition, the spectrum contained resonances at 2.24 (s, $ArC\mathit{H}_3$) due to 2,5-bis-[4′-(*n*-perfluoroheptyloctyloxy)benzoyloxy] toluene, and at 6.83 (s, $ArC\mathit{H}Br_2$) and 7.74 (m, 1 aromatic H *ortho* to $C\mathit{H}Br_2$) due to 2,5-bis[4′-(*n*-perfluoroheptyloctyloxy)-benzoyloxy] benzyl dibromide.

4.3.2. *Potassium n-alkanoates (n = 3–13)*

The potassium *n*-alkanoates were prepared in 75–93% yield as in the following example. A solution of propionic acid (0.46 g, 6.3 mmol) in methanol (5 ml) was titrated to a phenolphthalein endpoint with 1.5 M methanolic KOH (4.5 ml). The solution was concentrated to a slurry using a rotary evaporator, and then poured into cold ether (300 ml). The resulting precipitate was collected and dried to yield 0.66 g (93%) of potassium propionate as a light pink solid; m.p. > 300°C.

4.3.3. *2,5-Bis[4′-(n-perfluoroheptyloctyloxy)benzoyloxy]-benzyl n-alkanoates (n = 2–13)*

The 2,5-bis[4′-(*n*-perfluoroheptyloctyloxy)benzoyloxy]-benzyl *n*-alkanoates were prepared in 10–42% yield as in the following example. A solution of 2,5-bis-[4′-(*n*-perfluoroheptyloctyloxy)benzoyloxy] benzyl bromide (0.15 g, 0.11 mmol $ArCH_2Br$), potassium acetate (23 mg, 0.23 mmol) and TBAH (16 mg, 4.6 μmol) in THF (0.3 ml) and DMSO (0.03 μl) was heated at 60°C for 14 h. The reaction mixture was then poured into cold water (100 ml). The resulting precipitate was collected and dried *in vacuo* to yield 0.14 g (93%) of crude product. This crude product was passed through a short column of basic activated alumina using CH_2Cl_2 as the eluant. The solvent was removed using a rotary evaporator, and the resulting white solid purified by column chromatography using silica gel as the stationary phase and a gradient of CH_2Cl_2/hexanes as the eluant. The solvent was removed using a rotary evaporator, and the product recrystallized from a mixture of ethanol (20 ml) and toluene (5 ml) to yield 42 mg (28%) of 2,5-bis-[4′-(*n*-perfluoroheptyloctyloxy)benzoyloxy] benzyl acetate as white crystals. ^1H NMR: 1.42 (m, $[C\mathit{H}_2]_4$, 16 H), 1.62 (m, $C\mathit{H}_2CH_2CF_2$, 4 H), 1.85 (m, $C\mathit{H}_2CH_2O$, 4 H), 1.96 (s, $C\mathit{H}_3CO_2$), 2.07 (m, $C\mathit{H}_2CF_2$, 4 H), 4.05 (t, $OC\mathit{H}_2$, 4 H), 5.13 (s, $ArC\mathit{H}_2$), 6.98 (d, 4 aromatic H *ortho* to OCH_2), 7.29 (m, 3 aromatic H of central ring), 8.13 (dd, 4 aromatic H *ortho* to CO_2Ar). Anal. ($C_{53}H_{48}F_{30}O_8$) C, H: calcd 46.03, 3.50; found 45.81, 3.46%.

2,5-Bis[4′-(*n*-perfluoroheptyloctyloxy)benzoyloxy] benzyl propionate. ^1H NMR: 1.06 (t, $C\mathit{H}_3$), 1.39 (m, $[C\mathit{H}_2]_4$, 16 H), 1.62 (m, $C\mathit{H}_2CH_2CF_2$, 4 H), 1.84 (m, $C\mathit{H}_2CH_2O$, 4 H), 2.07 (m, $C\mathit{H}_2CF_2$, 4 H), 2.28 (q, $C\mathit{H}_2CO_2$), 4.05 (t, $OC\mathit{H}_2$, 4 H), 5.14 (s, $ArC\mathit{H}_2$), 6.98 (d, 4 aromatic H *ortho* to OCH_2), 7.29 (m, 3 aromatic H of central ring), 8.14 (dd, 4 aromatic H *ortho* to CO_2Ar). Anal. ($C_{54}H_{50}F_{30}O_8$) C, H: calcd 46.43, 3.61; found 46.34, 3.58%.

2,5-Bis[4′-(*n*-perfluoroheptyloctyloxy)benzoyloxy] benzyl *n*-butanoate. ^1H NMR: 0.87 (t, $C\mathit{H}_3$), 1.40 (m, $[C\mathit{H}_2]_4$, 16 H), 1.60 (m, $C\mathit{H}_2CH_2CO_2$), 1.65 (m, $C\mathit{H}_2CH_2CF_2$, 4 H), 1.82 (m, $C\mathit{H}_2CH_2O$, 4 H), 2.03 (m, $C\mathit{H}_2CF_2$, 4 H), 2.24 (t, $C\mathit{H}_2CO_2$), 4.05 (t, $OC\mathit{H}_2$, 4 H), 5.14 (s, $ArC\mathit{H}_2$), 6.98 (m, 4 aromatic H *ortho* to OCH_2), 7.29 (m, 3 aromatic H of central ring), 8.14 (dd, 4 aromatic H *ortho* to CO_2Ar). Anal. ($C_{55}H_{52}F_{30}O_8$) C, H: calcd 46.82, 3.71; found 46.90, 3.80%.

2,5-Bis[4′-(*n*-perfluoroheptyloctyloxy)benzoyloxy] benzyl *n*-pentanoate. ^{1}H NMR: 0.85 (t, $C\mathit{H}_3$), 1.27 (m, $C\mathit{H}_2CH_3$), 1.45 (m, $C\mathit{H}_2CH_2CO_2$ and $[C\mathit{H}_2]_4$, 18 H), 1.62 (m, $C\mathit{H}_2CH_2CF_2$, 4 H), 1.84 (m, $C\mathit{H}_2CH_2O$, 4 H), 2.06 (m, $C\mathit{H}_2CF_2$, 4 H), 2.25 (t, $C\mathit{H}_2CO_2$), 4.06 (t, $OC\mathit{H}_2$, 4 H), 5.13 (s, $ArC\mathit{H}_2$), 6.98 (d, 4 aromatic H *ortho* to OCH_2), 7.28 (m, 3 aromatic H of central ring), 8.13 (dd, 4 aromatic H *ortho* to CO_2Ar). Anal. ($C_{56}H_{54}F_{30}O_8$) C, H: calcd 47.20, 3.82; found 46.90, 3.72%.

The ^{1}H NMR spectra of the 2,5-bis[4′-(*n*-perfluoroheptyloctyloxy)benzoyoxy] benzyl *n*-alkanoates with $n = 6$–13 are identical: 0.86 (t, $C\mathit{H}_3$), 1.23 (m, $[C\mathit{H}_2]_{n\text{-}4}CH_3$), 1.45 (m, $C\mathit{H}_2CH_2CO_2$ and $[C\mathit{H}_2]_4$, 18 H), 1.62 (m, $C\mathit{H}_2CH_2CF_2$, 4 H), 1.84 (m, $C\mathit{H}_2CH_2O$, 4 H), 2.05 (m, $C\mathit{H}_2CF_2$, 4 H), 2.25 (t, $C\mathit{H}_2CO_2$), 4.06 (t, $OC\mathit{H}_2$, 4 H), 5.13 (s, $ArC\mathit{H}_2$), 6.98 (d, 4 aromatic H *ortho* to OCH_2), 7.28 (m, 3 aromatic H of central ring), 8.15 (dd, 4 aromatic H *ortho* to CO_2Ar). Anal. $n = 6$ ($C_{57}H_{56}F_{30}O_8$) C, H: calcd 47.58, 3.92; found 47.51, 3.97%. Anal. $n = 7$ ($C_{58}H_{58}F_{30}O_8$) C, H: calcd 47.94, 4.02; found 48.07, 4.10%. Anal. $n = 8$ ($C_{59}H_{60}F_{30}O_8$) C, H: calcd 48.30, 4.12; found 48.23, 4.08%. Anal. $n = 9$ ($C_{60}H_{62}F_{30}O_8$) C, H: calcd 48.66, 4.22; found 48.66, 4.22%. Anal. $n = 10$ ($C_{61}H_{64}F_{30}O_8$) C, H: calcd 49.00, 4.31; found 48.64, 4.23%. Anal. $n = 11$ ($C_{62}H_{66}F_{30}O_8$) C, H: calcd 49.34, 4.41; found 49.25, 4.33%. Anal. $n = 12$ ($C_{63}H_{68}F_{30}O_8$) C, H: calcd 49.68, 4.50; found 49.40, 4.32%. Anal. $n = 13$ ($C_{64}H_{70}F_{30}O_8$) C, H: calcd 50.01, 4.59; found 50.10, 4.62%.

Acknowledgment is made to the donors of The Petroleum Research Fund, administered by the American Chemical Society, for support of this research. C.P. also acknowledges the National Science Foundation for an NSF Young Investigator Award (1994–1999), and matching funds from Bayer, Dow Chemical, DuPont (DuPont Young Professor Grant), GE Foundation (GE Junior Faculty Fellowship), Pharmacia Biotech and Waters Corporation.

References

[1] (*a*) Demus, D., and Zaschke, H., 1984, *Flussige Kristalle in Tabellen II* (Leipzig: VEB Deutscher Verlag); (*b*) Gray, G. W., 1979, in *The Molecular Physics of Liquid Crystals*, edited by G. R. Luckhurst, and G. W. Gray (London: Academic Press), p. 1; (*c*) Ishizuka, H., Nishiyama, I., and Yoshizawa, A., 1995, *Liq. Cryst.*, **18,** 775.

[2] (*a*) Weissflog, W., and Demus, D., 1983, *Cryst. Res. Technol.*, **18,** K21; (*b*) Weissflog, W., and Demus, D., 1984, *Cryst. Res. Technol.*, **19,** 55.

[3] (*a*) Demus, D., Hauser, A., Isenberg, A., Pohl, M., Selbmann, C., Weissflog, W., and Wieczorek, S., 1985, *Cryst. Res. Technol.*, **20,** 1413; (*b*) Demus, D., Diele, S., Hauser, A., Latif, I., Selemann, C., and Weissflog, W., 1985, *Cryst. Res. Technol.*, **20,** 1547; (*c*) Rein, C., and Demus, D., 1993, *Liq. Cryst.*, **15,** 193.

[4] Ballauff, M., 1987, *Liq. Cryst.*, **2,** 519.

[5] (*a*) Young, W. R., and Green, D. C., 1974, *Mol. Cryst. liq. Cryst.*, **26,** 7; (*b*) Weissflog, W., Schlick, R., and Demus, D., 1981, *Z. Chem.*, **21,** 452; (*c*) Weissflog, W., and Demus, D., 1985, *Mol. Cryst. liq. Cryst.*, **129,** 235; (*d*) Weissflog, W., Wiegeleben, A., and Demus, D., 1985, *Mat. Chem. Phys.*, **12,** 461; (*e*) Imrie, C. T., and Taylor, L., 1989, *Liq. Cryst.*, **6,** 1; (*f*) Stützer, C., Weissflog, W., and Stegemeyer, H., 1996, *Liq. Cryst.*, **21,** 557.

[6] Arora, S. L., Fergason, J. L., and Taylor, T. R., 1970, *J. org. Chem.*, **35,** 4055.

[7] (*a*) Diele, S., Roth, K., and Demus, D., 1986, *Cryst. Res. Technol.*, **21,** 97; (*b*) Diele, S., Weissflog, W., Pelzl, G., Manke, H., and Demus, D., 1986, *Liq. Cryst.*, **1,** 101; (*c*) Perez, F., Berdagué, P., Judeinstein, P., Bayle, J. P., Allouchi, H., Chasseau, D., Cotrait, M., and Lafontaine, E., 1995, *Liq. Cryst.*, **19,** 345; (*e*) Berdagué, P., Perez, F., Bayle, J. P., Ho, M.-S., Fung, B. M., 1995, *New J. Chem.*, **19,** 383.

[8] (*a*) Takenaka, S., Masuda, Y., Iwano, M., Morita, H., Kusabayashi, S., Sugiura, H., and Ikemoto, T., 1989, *Mol. Cryst. liq. Cryst.*, **168,** 111; (*b*) Weissflog, W., Demus, D., and Diele, S., 1990, *Mol. Cryst. liq. Cryst.*, **191,** 9; (*c*) Berdague, P., Bayle, J. P., Ho, M.-S., and Fung, B. M., 1993, *Liq. Cryst.*, **14,** 667, and erratum 1995, *Liq. Cryst.*, **18,** 823.

[9] (*a*) Weissflog, W., and Demus, D., 1988, *Liq. Cryst.*, **3,** 275; (*b*) Hartung, H., Hoffmann, F., Stützer, C., and Weissflog, W., 1995, *Liq. Cryst.*, **19,** 839; (*c*) Stützer, C., Weissflog, W., and Stegemeyer, H., 1996, *Liq. Cryst.*, **21,** 557.

[10] Andersch, J., and Tschierske, C., 1996, *Liq. Cryst.*, **21,** 51.

[11] (*a*) Goodby, J. W., and Walton, C. R., 1985, *Mol. Cryst. liq. Cryst.*, **122,** 219; (*b*) Hsu, C.-S., Chu, P.-H., Chang, H.-L., and Hsieh, T.-H., 1997, *J. Polym. Sci., Polym. Chem. Ed.*, **35,** 2793.

[12] (*a*) Antoun, S., Lenz, R. W., and Jin, J.-I., 1981, *J. Polym. Sci., Polym. Chem. Ed.*, **19,** 1901; (*b*) Nieri, P., Ramireddy, C., Wu, C. N., Munk, P., and Lenz, R. W., 1992, *Macromolecules*, **25,** 1796.

[13] (*a*) Hudson, S. D., Lovinger, A. J., Larson, R. G., Davis, D. D., Garay, R. O., and Fujishiro, K., 1993, *Macromolecules*, **26,** 5643; (*b*) Caruso, U., Pragliola, S., Roviello, A., Sirigu, A., and Ianneli, P., 1995, *Macromolecules*, **28,** 6089; (*c*) Iannelli, P., Pragliola, S., Roviello, A., and Sirigu, A., 1997, *Macromolecules*, **30,** 4247.

[14] He, Z., Davis, F. J., and Mitchell, G. R., 1996, *Eur. Polym. J.*, **32,** 735.

[15] (*a*) Chang, S., and Han, C. D., 1996, *Macromolecules*, **29,** 2103; (*b*) Chang, S., and Han, C. D., 1997, *Macromolecules*, **30,** 1670.

[16] Caruso, U., Pragliola, S., Roviello, A., and Sirigu, A., 1993, *Macromolecules*, **26,** 221.

[17] Fujishiro, K., and Lenz, R. W., 1992, *Macromolecules*, **25,** 81.

[18] Reinitzer, F., 1888, *Monatsch Chem.*, **9**, 421.

[19] (*a*) Pugh, C., Arehart, S., Liu, H., and Narayanan, R., 1994, *J. macromol. Sci.—pure appl. Chem.*, **A31**, 1591; (*b*) Pugh, C., Liu, H., Arehart, S., and Narayanan, R., 1995, *Macromol. Symp.*, **98**, 293.

[20] Arehart, S. V., and Pugh, C., 1997, *J. Am. chem. Soc.*, **119**, 3027.

[21] For example, see the following papers and references therein: (*a*) Hessel, F., and Finkelmann, H., 1985, *Polym. Bull.*, **14**, 375; (*b*) Zhou, Q.-F., Li, H.-M., and Feng, X. D., 1987, *Macromolecules*, **20**, 233; (*c*) Keller, P., Hardouin, F., Mauzac, M., and Achard, M. F., 1988, *Mol. Cryst. liq. Cryst.*, **155**, 171; (*d*) Attard, G. S., Araki, K., Moura-Ramos, J. J., and Williams, G., 1988, *Liq. Cryst.*, **3**, 861; (*e*) Lewthwaite, R. A., Gray, G. W., and Toyne, K. J., 1992, *J. mater. Chem.*, **2**, 119; (*f*) Pugh, C., and Shrock, R. R., 1992, *Macromolecules*, **25**, 6593; (*g*) Percec, V., and Tomazos, D., 1993, *J. mater. Chem.*, **3**, 643; (*h*) Takenaka, S., and Yamasaki, Y., 1995, *Mol. Cryst. liq. Cryst.*, **258**, 51; (*i*) Leroux, N., and Chien, L.-C., 1996, *Liq. Cryst.*, **21**, 189; (*j*) Lecommandoux, S., Achard, M. F., Hardouin, F., Brulet, A., and Cotton, J. P., 1997, *Liq. Cryst.*, **22**, 549; (*k*) Pugh, C., Dharia, J., and Arehart, S. V., 1997, *Macromolecules*, **30**, 4520; (*l*) Pugh, C., Shao, J., Ge, J. J., and Cheng, S. Z. D., 1998, *Macromolecules*, **31**, 1779.

[22] (*a*) Pugh, C., and Kiste, A. L., 1997, *Prog. Polym. Sci.*, **22**, 601; (*b*) Pugh, C., and Kiste, A. L., 1998, *Handbook of Liquid Crystals*, edited by D. Demus, J. W. Goodby, G. W. Gray, H. W. Spiess and V. Vill, Vol. 3 (Weinheim: VCH), Chap.3.

[23] Christensen, J. J., Hanks, R. W., and Izatt, R. M., 1982, *Handbook of Heats of Mixing* (New York: Wiley).

[24] (*a*) Gray, G. W., and Goodby, J. W., 1984, *Smectic Liquid Crystals. Textures and Structures* (Glasgow: Leonard Hall); (*b*) Demus, D., and Richter, L., 1978, *Textures of Liquid Crystals* (Weinheim: Verlag Chemie).

[25] Pugh, C., Bae, V.-Y., Dharra, V., Ge, V. V., and Cheng, S. Z. D., 1998, *Macromolecules*, **31**, 5188.